Compañ Moreno, V.; Escorihuela Fuentes, J.; Olvera, J.; Garcia-Bernabe, A.; Andrio, A. (2020). Influence of the anion on diffusivity and mobility of ionic liquids composite polybenzimidazol membranes. Electrochimica Acta. 354:1-12. https://doi.org/10.1016/j.electacta.2020.136666

Supporting Information for

Influence of the anion on proton diffusivity and mobility of ionic liquids composite polybenzimidazol membranes

Jorge Escorihuela,[†,‡] *Jessica Olvera,*[§] *Andreu Andrio,*[‖] *Abel García-Bernabé,*[†] *and Vicente Compañ*,*[†]

† Departamento de Termodinámica Aplicada, Universitat Politècnica de València, Camino de Vera s/n, 46020 Valencia, Spain.

‡ Departament de Química Orgànica, Universitat de València, Av. Vicent Andrés Estellés s/n, 46100, Burjassot, Valencia, Spain; escorihu@uji.es (J.E)

§ Departamento de Polímeros del Instituto de Investigación en Materiales de la Universidad Autónoma de México (UNAM).

‖ Departamento de Física Aplicada, Universitat Jaume I, Avda. Sos Baynat, s/n, 12080, Castelló de la Plana, Spain

Full Gaussian citation:

Gaussian 16, Revision B.01, Frisch, M. J.; Trucks, G. W.; Schlegel, H. B.; Scuseria, G. E.; Robb, M. A.; Cheeseman, J. R.; Scalmani, G.; Barone, V.; Petersson, G. A.; Nakatsuji, H.; Li, X.; Caricato, M.; Marenich, A. V.; Bloino, J.; Janesko, B. G.; Gomperts, R.; Mennucci, B.; Hratchian, H. P.; Ortiz, J. V.; Izmaylov, A. F.; Sonnenberg, J. L.; Williams-Young, D.; Ding, F.; Lipparini, F.; Egidi, F.; Goings, J.; Peng, B.; Petrone, A.; Henderson, T.; Ranasinghe, D.; Zakrzewski, V. G.; Gao, J.; Rega, N.; Zheng, G.; Liang, W.; Hada, M.; Ehara, M.; Toyota, K.; Fukuda, R.; Hasegawa, J.; Ishida, M.; Nakajima, T.; Honda, Y.; Kitao, O.; Nakai, H.; Vreven, T.; Throssell, K.; Montgomery, J. A., Jr.; Peralta, J. E.; Ogliaro, F.; Bearpark, M. J.; Heyd, J. J.; Brothers, E. N.; Kudin, K. N.; Staroverov, V. N.; Keith, T. A.; Kobayashi, R.; Normand, J.; Raghavachari, K.; Rendell, A. P.; Burant, J. C.; Iyengar, S. S.; Tomasi, J.; Cossi, M.; Millam, J. M.; Klene, M.; Adamo, C.; Cammi, R.; Ochterski, J. W.; Martin, R. L.; Morokuma, K.; Farkas, O.; Foresman, J. B.; Fox, D. J. Gaussian, Inc., Wallingford CT, 2016.

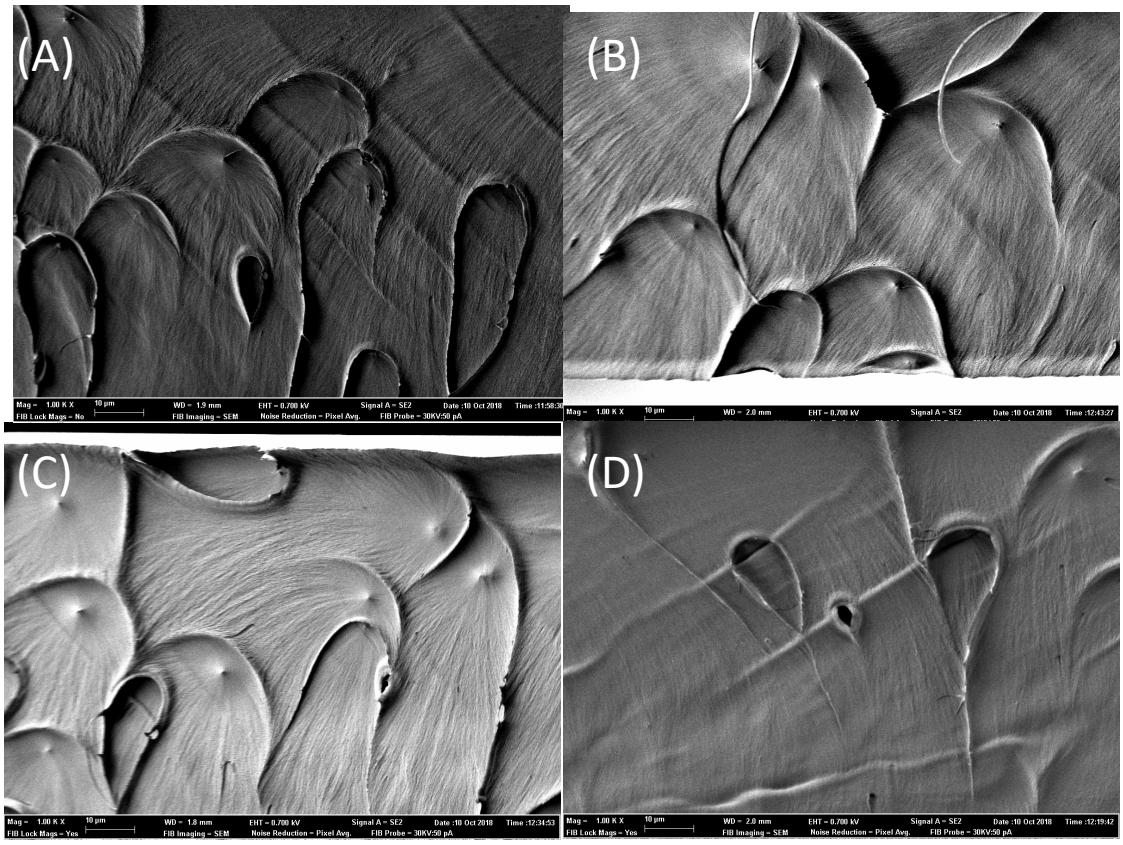

Figure S1. Cross-sectional SEM images of (A) PBI@BMIM-Cl, (B) PBI@BMIM-NTf_2, (C) PBI@BMIM-BF_4 and (D) PBI@BMIM-NCS.

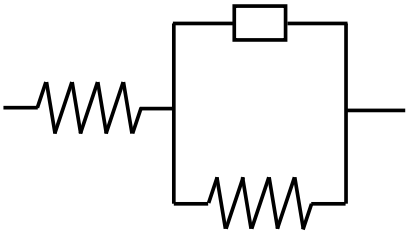

$$Z^*(\omega) = R_s + \frac{R_p}{1 + R_p Y_0 (j\omega\tau)^n}$$

Figure S2. Equivalent circuits that comprises a resistance R_s in series with a circuit made up of an element R_p representing the charge transfer resistance at the interface sample/electrode in parallel with a constant phase element (CPE), representing the sample/electrode double layer.

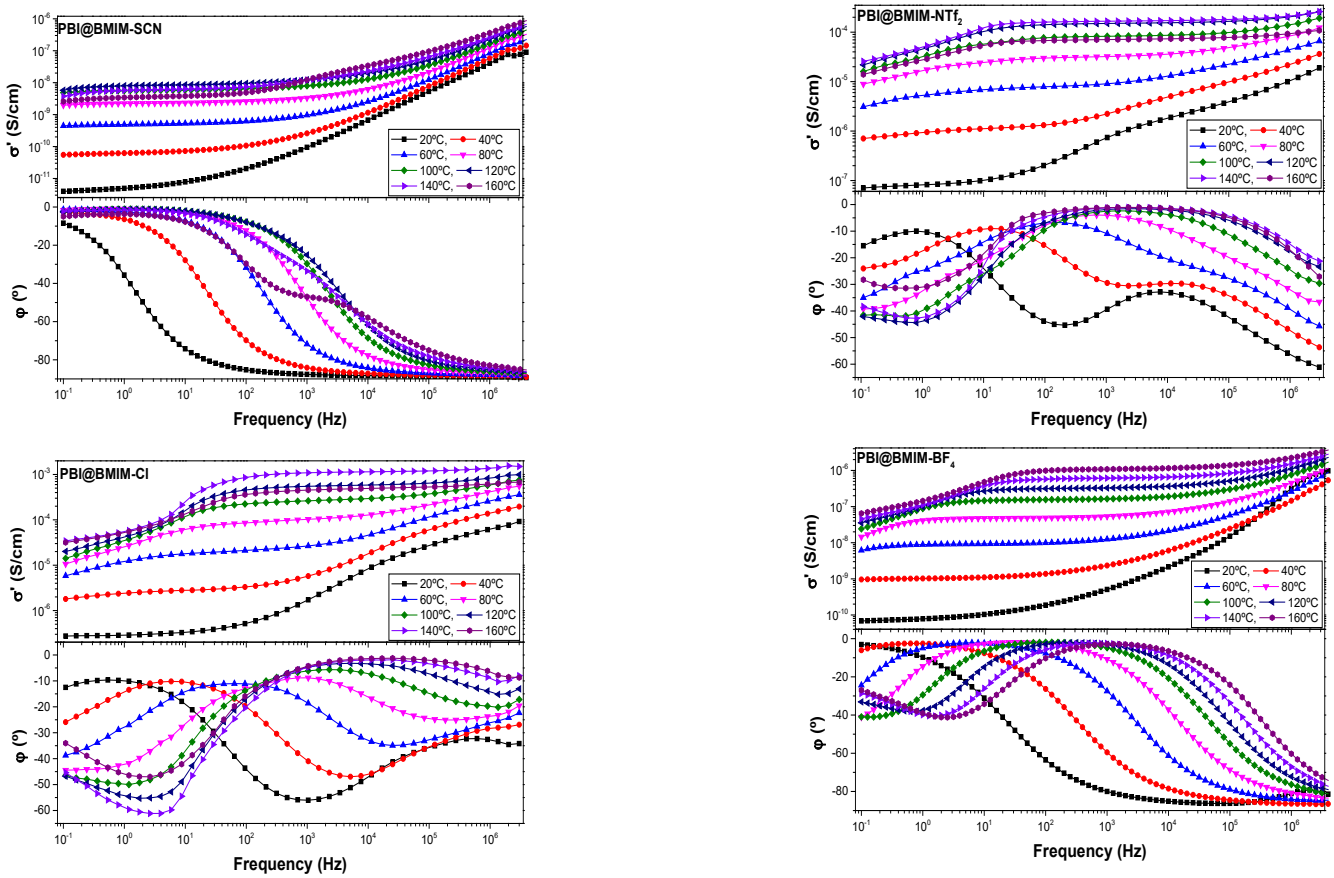

Figure S3. Bode diagram for PBI@BMIM-BF_4, PBI@BMIM-NCS, PBI@BMIM-NTf_2 and PBI@BMIM-Cl composite membranes at several temperatures.

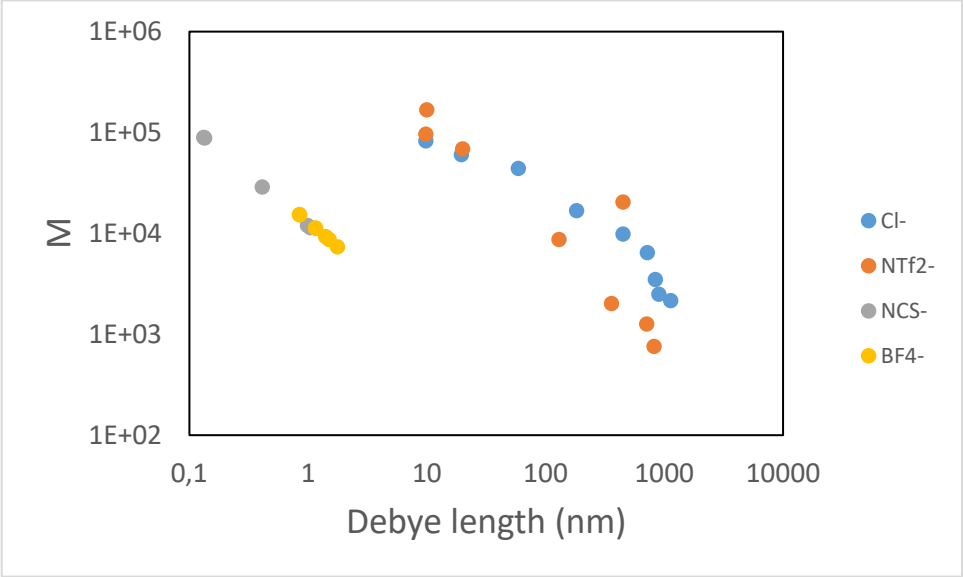

Figure S4. Variation of M parameter with Debye lenght for PBI@BMIM-BF_4, PBI@BMIM-NCS, PBI@BMIM-NTf_2 and PBI@BMIM-Cl composite membranes in all the range of temperatures.

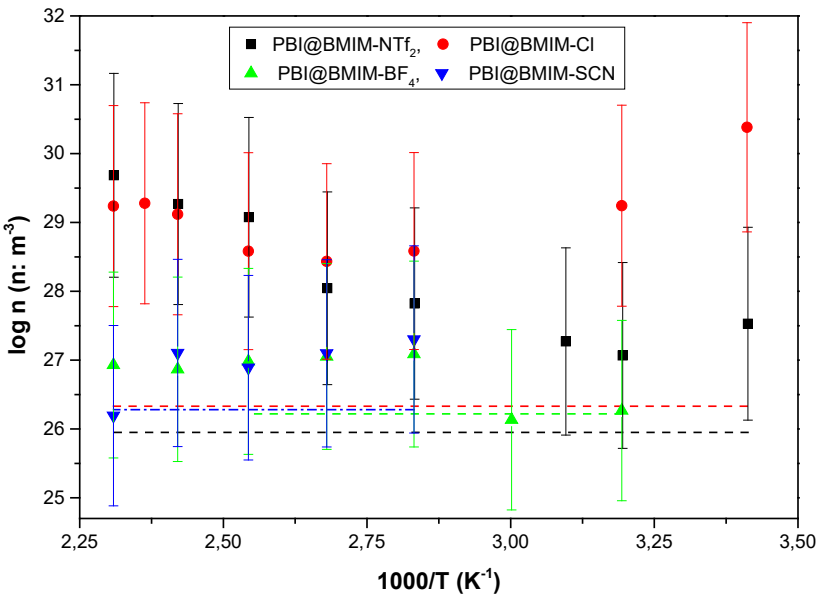

Figure S5. Mobile charge density for PBI@BMIM-BF_4, PBI@BMIM-NCS, PBI@BMIM-NTf_2 and PBI@BMIM-Cl composite membranes at several temperatures.

Table S1. Water uptake (%), swelling (%) and thickness uptake (%) of IL composite PBI membranes (containing 5 wt. % of BMIM-X) studied in this work.

Membrane	Water uptake (%)	Swelling (%)	Thickness uptake (%)
PBI	4 ± 1	5 ± 1	4 ± 1
PBI@BMIM-Cl	9 ± 1	7 ± 1	6 ± 1
PBI@BMIM-BF_4	7 ± 1	5 ± 1	4 ± 1
PBI@BMIM-NCS	8 ± 1	6 ± 1	5 ± 1
PBI@BMIM-NTf_2	9 ± 1	8 ± 1	7 ± 1

Table S2. Mechanical properties of IL composite PBI membranes (containing 5 wt. % of BMIM-X) studied in this work.

Membrane	Young's Modulus (GPa)	Tensile Stress (MPa)	Strain at break (%)
PBI	2.7 ± 0.8	100 ± 5	27 ± 2
PBI@BMIM-Cl	3.7 ± 0.2	143 ± 6	9 ± 1
PBI@BMIM-BF_4	2.9 ± 0.3	127 ± 5	17 ± 2
PBI@BMIM-NCS	3.5 ± 0.4	134 ± 4	10 ± 1
PBI@BMIM-NTf_2	3.2 ± 0.3	131 ± 4	19 ± 1